



A Dynamic Behaviour Analysis on the Frequency Control Capability of Electric Vehicles

Zarogiannis, Athanasios ; Marinelli, Mattia; Træholt, Chresten; Knezovic, Katarina; Andersen, Peter Bach

Published in:

Proceedings of International Universities' Power Engineering Conference (UPEC) 2014

Link to article, DOI:

[10.1109/UPEC.2014.6934763](https://doi.org/10.1109/UPEC.2014.6934763)

Publication date:

2014

[Link back to DTU Orbit](#)

Citation (APA):

Zarogiannis, A., Marinelli, M., Træholt, C., Knezovic, K., & Andersen, P. B. (2014). A Dynamic Behaviour Analysis on the Frequency Control Capability of Electric Vehicles. In Proceedings of International Universities' Power Engineering Conference (UPEC) 2014 IEEE. <https://doi.org/10.1109/UPEC.2014.6934763>

General rights

Copyright and moral rights for the publications made accessible in the public portal are retained by the authors and/or other copyright owners and it is a condition of accessing publications that users recognise and abide by the legal requirements associated with these rights.

- Users may download and print one copy of any publication from the public portal for the purpose of private study or research.
- You may not further distribute the material or use it for any profit-making activity or commercial gain
- You may freely distribute the URL identifying the publication in the public portal

If you believe that this document breaches copyright please contact us providing details, and we will remove access to the work immediately and investigate your claim.

A Dynamic Behaviour Analysis on the Frequency Control Capability of Electric Vehicles

Athanasios Zarogiannis, Mattia Marinelli, Chresten Træholt, Katarina Knezović, Peter Bach Andersen
Department of Electrical Engineering, Center for Electric Power and Energy, DTU - Technical University of Denmark
Contact person: Mattia Marinelli (matm@elektro.dtu.dk)

Abstract—The paper presents results of a study on the dynamic response of Electric Vehicle's (EV) when participating in frequency control of an islanded system. The following cases were considered: when there is no EV performing frequency control, when the EV participates in primary frequency control and when the EV participates in both primary and secondary frequency control. Different parameters are tested in various combinations, and their influence on frequency deviation as well as power and energy provided by the EV with vehicle-to-grid (V2G) capability is shown.

Index Terms—Electric vehicles, island operation, load frequency control, primary frequency control, V2G

I. INTRODUCTION

The increasing percentage of renewable energy sources (RES) in the power production results in growing amount of fluctuating active power injected into the transmission and distribution grids. This leads to imbalances and consequently the need for additional control reserves to ensure the balance between production and consumption. Small islanded systems will be highly affected by such power imbalances and as a result, the frequency can suffer severe fluctuations [1], [2]. An example of an islanded system is a micro-grid detached from the main grid or operated as an autonomous system. In such system, the frequency is more sensitive to changes in power balance (e.g. power deficit). This may lead to limitations on the percentage of RES penetration in islanded systems and ultimately also in larger power systems. Adding electric vehicles (EVs) with uncontrolled charging schemes can cause even larger imbalances in the system.

Control measures can be taken by loads the same way as they are taken by generating units. Electric vehicles with Vehicle-to-Grid (V2G) capability can be considered as controllable loads which may respond to frequency variations with the following advantages [3]:

- 1) A large number of small loads can provide ancillary services more reliably than a few large generators where a failure has a more significant impact [4].
- 2) EVs have the capability of charging/discharging their power very quickly responding to an operator's requests almost instantaneously.

- 3) The distribution of EVs throughout the grid allows them to act like mobile power plants if considered in groups [5].

In [6], resources scheduling scenarios under uncertainty in a smart grid, with renewables and plug-in electric vehicles was analysed. In [7], a control strategy is proposed for a solar power based micro-grid, combining solar generation during the day with night consumption delivered by EVs using the V2G concept. Moreover, a comparative study is performed in [8] in order to quantify the amount of wind power that can be integrated in an isolated electricity grid if EVs are used only as dumb loads and if EVs participate in frequency control.

It is argued that EVs with V2G capability can provide regulation services and can compete in electricity markets, such as markets for ancillary services, where there is payment for available capacity apart from the payment for the actual dispatch. Frequency control is one of the services which can be provided by EVs through this market [6]. More specifically, Primary Frequency Control (PFC) can be suitably provided by EVs, due to their flexible operating mode and ability to seamlessly alter the consuming/producing power under the V2G concept [9]. Since a single vehicle is too small to provide regulation alone, an aggregator must gather a considerable amount of EVs and act as a Virtual Power Plant [10], [11].

Frequency reserves provided by EVs can additionally be used in secondary frequency control or Load Frequency Control (LFC), which is also a part of the automatic control system together with PFC. The task of PFC is to bring the frequency back to acceptable values in the short term leaving a frequency error due of the fully proportional control law. LFC has the task to compensate for the remaining frequency error after the primary control has acted and to ensure the same frequency levels between interconnected systems. Thus, it releases the primary control and takes into account the changes in the load flows [12].

This paper presents the impact that V2G has on the frequency when operated in an islanded system. The participation of the EV in PFC as well as in LFC is studied and results regarding the behaviour of system frequency as well as the active power and energy provided by the EVs are presented.

II. METHODOLOGY

A. Network Model

This paper presents the results of a study performed in Matlab-SimPowerSystems regarding the influence of EVs with V2G capability participating in frequency control of an islanded system. A single busbar system is used for evaluating the capability of EVs to perform frequency control. The 10 kV busbar is connected to a 100 kW synchronous generator which includes a simple hydraulic governor and an excitation system as described in [12]. The overall machine inertia is equal to 3 seconds. A 10kV/0.4kV transformer is used to connect the generator with the rest of the network. A static load is connected to the system and the frequency dynamic is triggered by an increase in the load set-point. Table I shows the model characteristics in terms of generation and load sizes.

TABLE I
PARAMETERS OF GRID COMPONENTS

| Generation/loads | Power (kW) |
|---|------------|
| Synchronous generator (P_{gen}) | 100 |
| Initial load at steady-state (P_{load}) | 50 |
| Load connected after 10 sec (ΔP_{load}) | 5 |

B. EV frequency control

The single EV considered in the system has V2G capability enabling it to inject power back to the grid if needed. Thus, the EV battery is simulated as controllable load connected to the system which can either absorb power in case of frequency rise or inject power in case of frequency drop. It is assumed that the EV is three-phase connected and initially is not charging. As a result, the EV load is set to 0 at the start of the simulation.

To manage EV output, frequency, which is an instantaneous indication of the power balance in the island network, is used to adapt the charging/discharging of the EV battery [8]. A frequency control droop loop is adopted to adjust the active power set-point of the battery as shown in Fig. 1.

The EV frequency control consists of the droop control and a simplified battery inverter component. The droop control includes the droop gain which gets the deviation in frequency as an input and gives the change in EV's power level as an output. Blocks of time delays are included in both components simulating the latency in the transfer of the frequency signal.

The battery inverter model includes a saturation block with upper and lower limits that imposes a restriction on the maximum amount of active power which can be exchanged between the EV and the grid. This limit depends on the capacity of the charging infrastructure that the EV is connected to. A limit is also imposed on the EV's rate for either absorbing or injecting active power. Another time delay is included in the inverter component in order to simulate the delay occurring

during the transformation of the signal from droop control to actual change in power level of the battery.

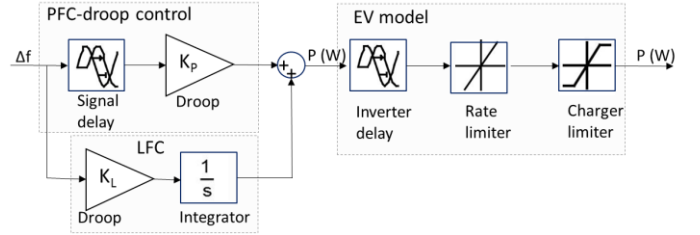


Fig. 1. PFC and LFC control loop and EV model.

Transient droop compensation used for emulating inertial response is also studied in this paper. This is accomplished by a transient gain reduction compensation which can be connected in series to the droop control and has the transfer function:

$$R_T \frac{sT_R}{1 + sT_R} \quad (1)$$

where R_T and T_R are temporary droop and reset time respectively [14]. Their initial values are given in Table II. The optimal combination of these values is chosen based on their impact on system frequency.

The EV participation in secondary control is also studied. For this reason, a secondary control component is added to the output of the droop control (PFC) as shown in Fig. 1. The input for the secondary control is again the frequency change compared to nominal value, which is then integrated and added to the output signal of the PFC. Table II shows the parameters of the frequency control components.

TABLE II
PARAMETERS OF EV FREQUENCY CONTROL COMPONENTS

| Components of Frequency Control | |
|---------------------------------|----------|
| Droop (%) | 10/7/5/2 |
| Signal delay(sec) | 1/2/3/4 |
| Saturation limit (kW) | 3 |
| Rate limiter (kW/sec) | 1 |
| Inverter delay (sec) | 1 |
| Temporary droop R_T | 0.4 |
| Reset time T_R (sec) | 5 |

C. Scenarios

The different scenarios analysed are:

- No EV contributes to frequency control
- EV participating in primary frequency control
- EV participating in primary and secondary frequency control

III. RESULTS ANALYSIS

Dynamic simulations are performed for the described scenarios. EV participation in PFC is studied under different value combinations for certain parameters, namely the droop value, the inertia of the machine connected to the system and the delay in signal transmission to droop control. These parameters are considered to be critical for the influence of EV in PFC. Table III contains the synthetic overview of the steady-state frequency and the maximum rate of change of frequency (ROCOF), with different combinations of signal delay and machine inertia. In these combinations, the droop is set to 5%. Two ROCOF are calculated: the first one is the frequency drop in the first 0.1 seconds after the contingency while the second one is the frequency drop evaluated in the time window between 1 and 1.1 seconds. Fig. 2 and Fig. 3 illustrate the minimum frequency (nadir) and the total energy provided by the EV battery to the system during the simulation period respectively. It can be observed that without the EV participation in PFC, the steady-state frequency is higher than when the EV participates.

TABLE III
RESULTS FOR DIFFERENT SIGNAL DELAY AND MACHINE INERTIA VALUES

| Delay (s) | Inertia (sec) | Steady state (Hz) | Steady state > 49 Hz | ROCOF @ 0.1s (Hz/s) | ROCOF @ 1s (Hz/s) |
|-----------|---------------|-------------------|----------------------|---------------------|-------------------|
| No EV | | 49.89 | yes | -0.41 | -0.46 |
| 1.00 | 1.50 | unstable | no | -0.81 | -1.04 |
| | 3.00 | 49.80 | yes | -0.41 | -0.46 |
| | 4.00 | 49.81 | yes | -0.31 | -0.34 |
| | 5.00 | 49.83 | yes | -0.25 | -0.26 |
| 2.00 | 1.50 | unstable | no | -0.81 | -1.04 |
| | 3.00 | 49.80 | yes | -0.41 | -0.46 |
| | 4.00 | 49.81 | yes | -0.31 | -0.34 |
| | 5.00 | 49.82 | yes | -0.25 | -0.26 |
| 3.00 | 1.50 | unstable | no | -0.81 | -1.04 |
| | 3.00 | 49.77 | yes | -0.41 | -0.46 |
| | 4.00 | 49.81 | yes | -0.31 | -0.34 |
| | 5.00 | 49.82 | yes | -0.25 | -0.26 |
| 4.00 | 1.50 | unstable | no | -0.81 | -1.05 |
| | 3.00 | 49.71 | yes | -0.41 | -0.46 |
| | 4.00 | 49.83 | yes | -0.31 | -0.34 |
| | 5.00 | 49.81 | yes | -0.20 | -0.22 |

Furthermore, in case of the machine inertia reduction from its initial value of 3 seconds to 1.5 seconds, meaning the machine is less capable of counteracting frequency changes, the system becomes unstable. This points out the incapability of the EV to have the primary role in frequency control. An increase in machine inertia to 5 seconds leads to higher steady-state frequency values. In all cases, except those of instability in the system, frequency is brought back to values very close to

nominal. ROCOF is higher for smaller values of machine inertia while it is not influenced by changes in signal delay values. ROCOF after the 1st second of the contingency is higher than ROCOF at the first 0.1 seconds.

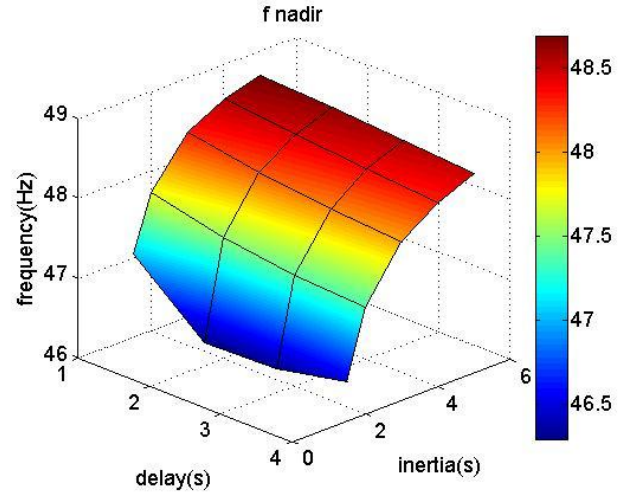


Fig. 2. Frequency nadir provided by the EV for different signal delay and machine inertia values.

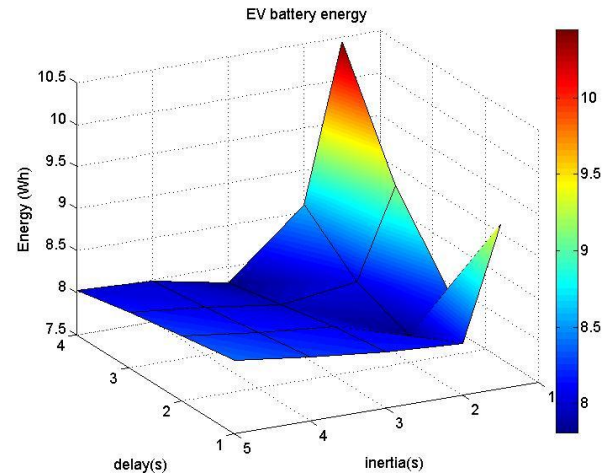


Fig. 3. Total energy provided by the EV for different signal delay and machine inertia values.

Fig. 2 shows that frequency nadir reaches its minimum value for higher signal delays and the machine inertia value of 1.5 second. In this case frequency drops down to less than 46.5 Hz while in cases where machine inertia is 4 or 5 seconds, it drops down to only around 48.5 Hz. The energy provided by the EV to the grid is significantly higher in case of low machine inertia due to the instability of the system, as shown in Fig. 3. In case of a stable system, the EV injects around 8.5 Wh to the grid.

Results for combination of different signal delay and droop values are presented in Table IV, Fig. 4 and Fig. 5. Machine inertia is set to 3 seconds. With no EV participation in PFC,

steady-state frequency is higher than with EV participation. A droop value of 2% results in lower steady-state value while in case of 3 seconds of signal delay, the system becomes unstable. It can be pointed out that the influence of signal delay and droop values on steady-state frequency is quite small, while ROCOF remains stable at -0.41 Hz/sec and -0.46 Hz/sec respectively, for all different cases.

TABLE IV
RESULTS FOR DIFFERENT SIGNAL DELAY AND DROOP VALUES

| Delay (s) | Droop (%) | Steady state (Hz) | ROCOF @0.1s (Hz/s) | ROCOF @1s (Hz/s) |
|-----------|-----------|-------------------|--------------------|------------------|
| No EV | | 49.89 | -0.41 | -0.46 |
| 1.00 | 10.00 | 49.84 | -0.41 | -0.46 |
| | 7.00 | 49.82 | -0.41 | -0.46 |
| | 5.00 | 49.80 | -0.41 | -0.46 |
| | 2.00 | 49.76 | -0.41 | -0.46 |
| 2.00 | 10.00 | 49.84 | -0.41 | -0.46 |
| | 7.00 | 49.82 | -0.41 | -0.46 |
| | 5.00 | 49.80 | -0.41 | -0.46 |
| | 2.00 | 49.74 | -0.41 | -0.46 |
| 3.00 | 10.00 | 49.84 | -0.41 | -0.46 |
| | 7.00 | 49.81 | -0.41 | -0.46 |
| | 5.00 | 49.77 | -0.41 | -0.46 |
| | 2.00 | unstable | -0.41 | -0.46 |
| 4.00 | 10.00 | 49.84 | -0.41 | -0.46 |
| | 7.00 | 49.81 | -0.41 | -0.46 |
| | 5.00 | 49.71 | -0.41 | -0.46 |
| | 2.00 | 48.70 | -0.41 | -0.46 |

Frequency nadir values vary from 48 to 48.5 Hz as shown in Fig. 4. Total energy provided by EV battery varies a lot: from 4 Wh for a droop of 10% to around 16 Wh for a droop of 2% as shown in Fig. 5. Change in signal delay values does not influence the total energy provided, since it just postpones the injection of EV power into the system. Fig. 6, Fig. 7 and Fig. 8 illustrate the change in frequency and in power and the energy provided by the EV throughout the simulation.

The cases of no EV in the system and EV participating in PFC with droop values 5% and 2% respectively are chosen to be compared. Machine inertia is set to 3 seconds and total delay is 2 seconds.

System reaction to contingency is better in case of EV participating in PFC, both in terms of maximum frequency drop and restoration of frequency back to acceptable levels. It can be observed that a 2% droop value results in oscillations in frequency due to the high amount of power contributed by EV. In this case, active power is limited to 3 kW because of the chargers limited capacity. In terms of energy, 2% droop results in double amount of energy provided by the EV.

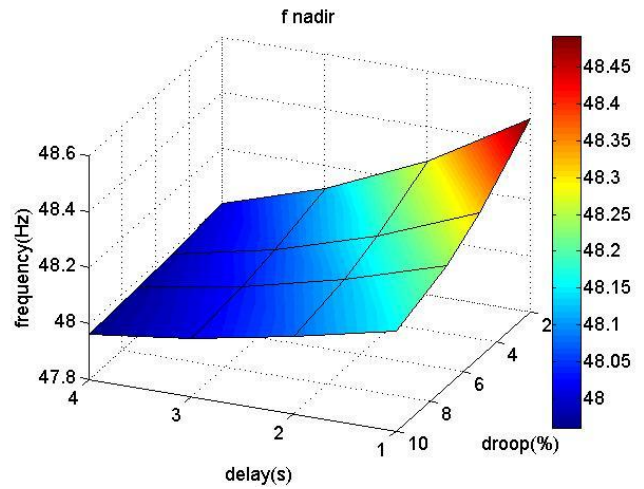


Fig. 4. Frequency nadir provided by the EV for different signal delay and droop values.

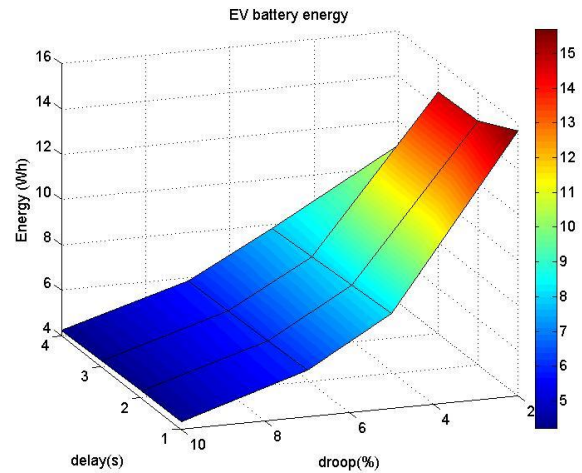


Fig. 5. Total energy provided by EV for different signal delay and droop values.

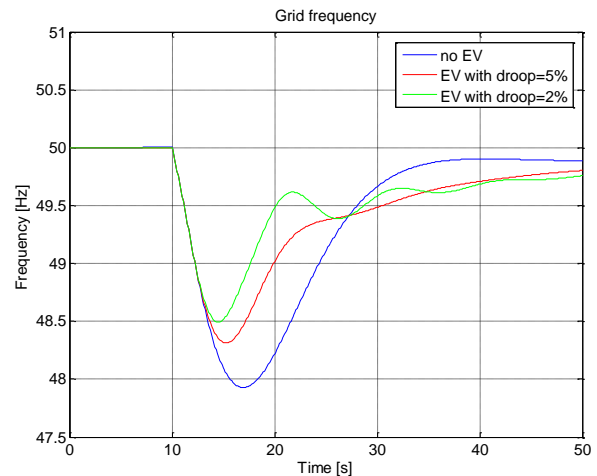


Fig. 6. Frequency drop in cases with no EV in PFC and with the EV having different droop values.

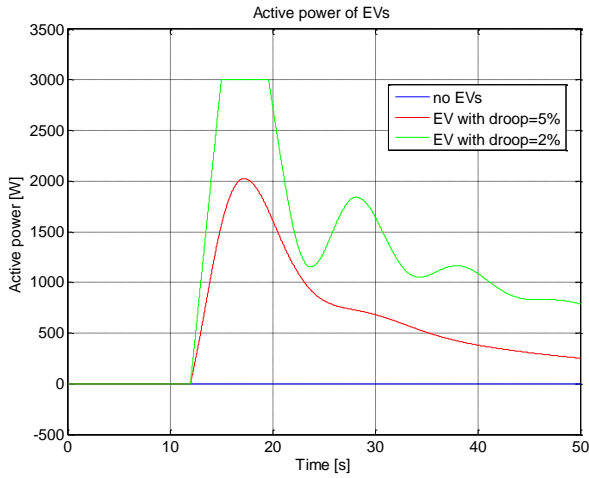


Fig. 7. Power provided by the EV in cases with no EV in PFC and with the EV having different droop values.

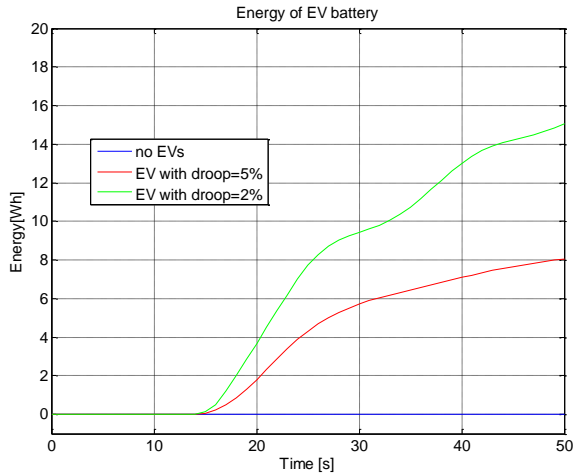


Fig. 8. Power provided by the EV in cases with no EV in PFC and with the EV having different droop values.

The effect of transient droop compensation on the frequency and the power provided by the EV is shown in Fig. 9 and Fig. 10, where different sets of parameters are illustrated.

The implementation of the transient droop results in a smoother curve and elimination of the oscillations occurring in the 2% droop case. On the other hand, the response of the EV frequency control component becomes slower, and maximum frequency drop is even higher than in case of 5% droop. The initial set of values ($T_R=10$ sec and $R_T=0.4$) was found to be the optimal combination with the criteria of maximum frequency drop and high steady-state frequency. Power provided by the EV does not display any oscillations in the case of transient droop compensation. It is worth noticing the need for power absorption from the EV after the first seconds of connecting the load. This leads to a smoother operation of the EV battery but the change from discharging to charging mode results in battery

degradation. Maximum power is lower reaching 2 kW at the time of maximum frequency drop.

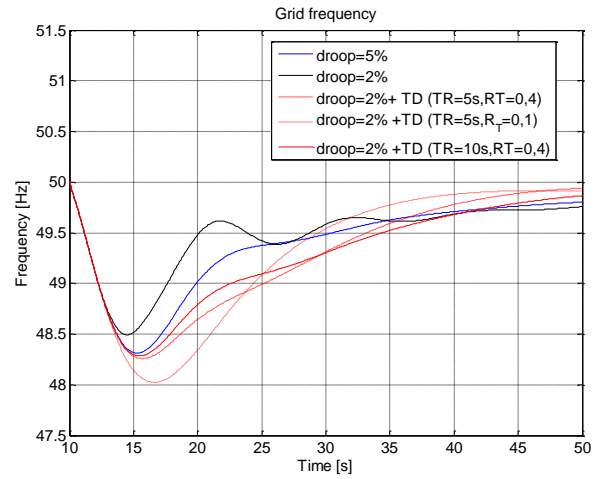


Fig. 9. Effect of transient droop compensation on frequency for different sets of T_R and R_T values.

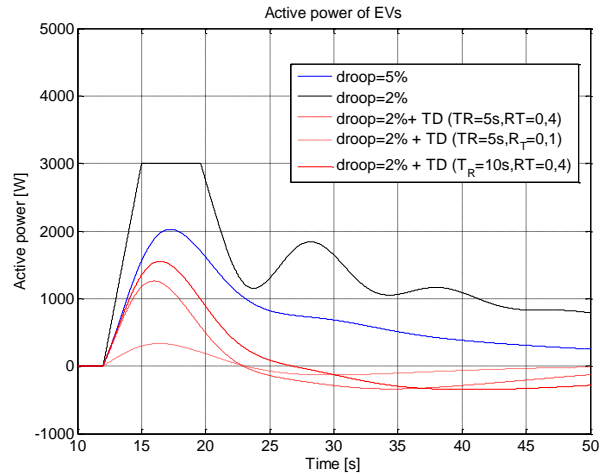


Fig. 10. Effect of transient droop compensation on power provided by EV for different sets of T_R and R_T values.

Fig. 11 shows the effect on frequency of LFC performed by EV in addition to PFC. The frequency drop is compared for 3 cases, namely no EV in PFC, EV participation in PFC and EV participation in PFC and LFC. Table V highlights the effect of LFC performed by the EVs in steady-state frequency and in energy provided from the EV battery to the grid.

In case of EV participating in LFC, frequency not only returns to a steady-state closer to nominal value but also recovers faster. In this case the energy required by the EV both for PFC and LFC is almost double the energy required when the EV participates only in PFC.

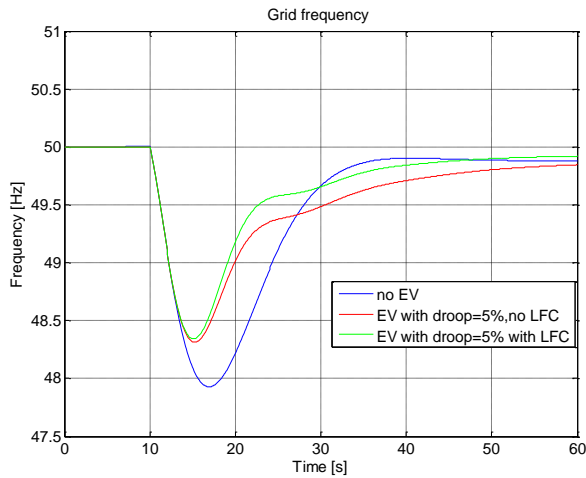


Fig. 11. Effect of LFC performed by EV on frequency drop.

TABLE V
RESULTS FOR LFC PERFORMED BY EV

| | Steady-state (Hz) | Energy provided by EV (Wh) |
|-------------|-------------------|----------------------------|
| only PFC | 49.85 | 8.2 |
| PFC and LFC | 49.92 | 15.6 |

IV. CONCLUSIONS

The aim of this paper is to analyse the frequency response in an islanded system where an EV with V2G capability participates in the frequency control. PFC as well as LFC performed by the EV resulted in a smoother frequency drop with lower maximum drop compared to no EV participation. Reducing the inertia of the machine led to instability in the system showing that the EV cannot perform frequency control as a stand-alone component using a traditional frequency control. Among different droop values tested, 5% droop resulted in optimal performance of EV control as it does not require high amount of power provided instantaneously by the EV battery and it does not create any oscillations in the frequency. Specific focus has been given also to the influence of delays in the frequency signal.

The results show that the delay in the frequency signal used for activating the primary frequency control is more important than the droop value of the controller itself. This aspect will be extremely important when evaluating the effective participation of an EV in providing frequency regulation. An experimental validation of the influence of the signal delay is currently in progress in the SYSLAB PowerLabDK laboratory at DTU.

Future works will include also the improvement of LFC, adding the ability to control the EV battery contribution to the system based on available energy for frequency regulation which is set by the EV user.

REFERENCES

- [1] F. Baccino, M. Marinelli, S. Massucco, and F. Silvestro, "Low voltage microgrid under islanded operation: Control strategies and experimental tests," *Power Generation, Transmission, Distribution and Energy Conversion (MEDPOWER 2012)*, 8th Mediterranean Conference on, pp.1-7, Cagliari, 1-3 Oct. 2012.
- [2] Y. Zoka, R. Tonoda, Y. Mashima, Y. Sasaki, and N. Yorino, "An on-demand control system for demand and supply control of small independent power grids," *Universities Power Engineering Conference (UPEC)*, 2012 47th International, pp.1-6, London, 4-7 Sept. 2012
- [3] W. Kempton and J. Tomic, "Vehicle-to-grid power implementation: from stabilizing the grid to supporting large scale renewable energy", *Journal of Power Sources*, 2005, Volume 144, Issue 1, pp 280-294.
- [4] B. Kirby, 'Spinning reserve from responsive loads', Oak Ridge National Laboratory, Oak Ridge, TN, Tech. Rep. ORNL/TM-2003/19, March 2003.
- [5] P. Baboli, M. Moghaddam, F. Fallahi, "Utilizing Electric Vehicles on Primary Frequency Control in Smart Power Grids," *IPCBE vol. 26 2011-International Conference on Petroleum and Sustainable Development, Singapore*, 2011.
- [6] A. Y. Saber and G.K. Venayagamoorthy, "Resource scheduling under uncertainty in a smart grid with renewables and plug-in vehicles," *IEEE Journal of Systems*, vol 6, no 1, pp 103-109, March 2012.
- [7] L. Udawatta, U. Madawala, D. Muthumuni, M. Vilathgamuwa, "Control of Solar Powered Micro-grids Using Electric Vehicles," *IEEE ICSET 24-27 September 2012, Nepal*.
- [8] J.A. Pecos Lopes, F.J. Soares, P.M. Rocha Almeida, "Using Vehicle-to-Grid to Maximize the Integration of Intermittent Renewable Energy Resources in Islanded Electric Grids," *ICCEP 2009-International Conference on Clean Electrical Power Renewable Energy Resources Impact, Capri, Italy*, 9-11 June, 2009.
- [9] C. Gouveia, C. Moreira, J. Lopes, D. Varajao, and R. Araujo, "Microgrid Service Restoration: The Role of Plugged-in Electric Vehicles," *Industrial Electronics Magazine, IEEE*, vol.7, no.4, pp.26-41, Dec. 2013.
- [10] F. Marra, D. Sacchetti, A.P. Pedersen, P.B. Andersen, C. Træholt, and E. Larsen, "Implementation of an Electric Vehicle test bed controlled by a Virtual Power Plant for contributing to regulating power reserves," *Power and Energy Society General Meeting, 2012 IEEE*, pp.1-7, San Diego, 22-26 July 2012.
- [11] L. Carradore, and R. Turri, "Electric Vehicles participation in distribution network voltage regulation," *Universities Power Engineering Conference (UPEC)*, 2010 45th International, pp.1-6, Cardiff, 31 Aug. – 3 Sept. 2010.
- [12] Avramiotis-Falireas N., 2012, "Indirect control of electric vehicles for the provision of secondary frequency control," Semester thesis, ETH-Power Systems Laboratory
- [13] P. Kundur, 'Power System Stability and Control', McGraw-Hill Inc., New York, 1994
- [14] M. Marinelli, S. Massucco, A. Mansoldo, and M. Norton, "Analysis of inertial response and primary frequency power control provision by doubly fed induction generator wind turbines in a small power system", *17th Power System Computation Conference (PSCC)*, pp. 1-7, Stockholm, 22-26 Aug. 2011.